

Surface-Induced Transformations for Surfactant Aggregates

Reuben E. Lamont[†] and William A. Ducker^{*,†}

Contribution from the Departments of Chemistry, University of Otago, Dunedin, New Zealand, and Virginia Polytechnical Institute and State University, Blacksburg, Virginia 24061-0212

Received December 18, 1997

Abstract: Hexadecyltrimethylammonium cations (CTA⁺) form ordered structures at the interface between muscovite mica and aqueous solution. The structure is altered in the sequence bilayer → ordered cylinder → disordered cylinder → short cylinder → sphere by successive addition of Cs⁺, that is, more curved structures are observed at higher salt concentrations. Parts of the same sequence occur at the interface on addition of other alkali cations, but the structure is more curved in the order Li⁺ < K⁺ < Cs⁺, following the softness of the ion. On addition of salt, the changes in aggregate shape at the interface occur in the opposite sequence to those that occur in bulk solution, demonstrating the dominance of surface interactions in this system. Substitution of a counterion that has a greater binding affinity for the CTA⁺ ion, Br⁻ for Cl⁻, leads to lower curvature structures at the same CTA⁺ and alkali cation concentrations. The effect of the counterion is similar to that observed in bulk, and is explained by a decrease in cation–cation repulsion in the presence of counterions that bind more strongly to the surfactant ion. The effect of rival cations can be explained by their binding affinity for the anionic mica substrate. The surface of muscovite mica has one negative charge per 0.48 nm². The high charge density induces a high density of surfactant cations, and thus low-curvature aggregates at the interface. When rival cations occupy these sites, the availability of surface counterions for the surfactant is reduced, and the aggregate curvature increases. The strength of this effect follows the softness of the ion, which we correlate with the relative binding affinity of the alkali metals for the mica/surfactant film compared to bulk water.

Introduction

Surfactants form aggregates in aqueous solution because of the low energy of interaction between water and the surfactant hydrocarbon chain (the hydrophobic effect), but the association is limited to finite dimensions mainly because of repulsive interactions between the surfactant headgroups. The observed curvature of surfactant aggregates has been rationalized by considering intermolecular forces, particularly in terms of the effective area of surfactant headgroup that is available to encapsulate a volume of surfactant hydrocarbon (the packing parameter model).¹ For ionic surfactants, the aggregate curvature decreases as salt is added to solution. This has been explained in terms of an increase in counterion association that reduces repulsive Coulombic forces between the charged headgroups, and favors a smaller area per charge and thus a less curved structure. The curvature of an ionic surfactant-aggregate can thus be tuned by altering the binding affinity or concentration of available counterions. For example, when NaBr is added to hexadecyltrimethylammonium bromide (CTAB), the surfactant aggregates undergo transitions in the order globular micelle → cylindrical micelle → wormlike micelle with increasing concentration.² Similar transitions occur for CTAC on addition of Cl⁻,³ but the transitions are shifted to higher concentration of anion, because the harder Cl⁻ ion has relatively greater affinity for water than for the quaternary ammonium ion.

Ionic surfactants form aggregates at interfaces for the same reason as they aggregate in bulk: because of the low energy of interaction between the hydrocarbon tail and water. However, the factors influencing the shape of the aggregates are not yet fully understood. It is reasonable to expect that counterions at the aggregate–solution interface have the same effect as those in bulk solution: a higher density of bound counterions leads to a lower-curvature aggregate.⁴ However, in this paper, we show that the addition of salt causes a sequence of transitions at the interface between muscovite mica and aqueous solution, which includes the same structures as in bulk solution, but with the opposite dependence on salt concentration. That is, transitions from bilayer → long, ordered cylinders → disordered cylinders → short cylinders → spheres occur as the salt concentration is increased. We explain these transitions in terms of a decreased density of *surface* counterions that are available to the surfactant when rival ions of the same charge as the surfactant are introduced. The concomitant introduction of additional counterions is a secondary influence.

In this paper we examine the influence of salt on the shape of surfactant aggregates at an interface using Atomic Force Microscopy (AFM).⁵ AFM was first used to image surfactant surface-aggregates by Manne *et al.*⁶ and has subsequently been used to study the adsorption of hexadecyltrimethylammonium chloride,⁷ tetradecylammonium bromide,⁸ and dodecyltrimethyl-

* Address correspondence to this author Virginia Polytechnical Institute.

[†] University of Otago.

(1) Israelachvili, J. N.; Mitchell, D. J.; Ninham, B. W. *J. Chem. Soc., Faraday Trans.* **1976**, *72*, 1525–1568.

(2) Vinson, P. K.; Bellare, J. R.; Davis H. T.; Miller, W. G.; Scriven, L. E. *J. Colloid. Interface Sci.* **1991**, *142*, 74–91.

(3) Imae, T.; Abe, A.; Ikeda, S. *J. Phys. Chem.* **1988**, *92*, 1548–1553.

(4) Ducker, W. A.; Grant, L. M. *J. Phys. Chem.* **1996**, *100*, 11507–11511.

(5) Binnig, G.; Quate, C.; Gerber, G. *Phys. Rev. Lett.* **1986**, *56*, 930–933.

(6) Manne, S.; Cleveland, J. P.; Gaub, H. E.; Stucky, G. D.; Hansma, P. K. *Langmuir* **1994**, *10*, 4409–4413.

(7) Aksay, I. A.; Trau, M.; Manne, S.; Monma, I.; Yao, N.; Zhou, L.; Fenter, P.; Eisenberger, P. M.; Gruner, S. M. *Science* **1996**, *273*, 982–998.

ammonium bromide⁹ to the mica–solution interface. For all three surfactants, cylindrical aggregates were observed. The adsorption of Gemini surfactants has also been studied,¹⁰ and the role of mica in orienting surface aggregates has been discussed.¹¹ The interface we have studied is the boundary between muscovite mica and CTA⁺ solutions that are above the critical micelle concentration (cmc). Chen et al. have examined the adsorption of CTA⁺ to mica by X-ray Photoelectron Spectroscopy (XPS).¹² Their principle finding was that the surface film was slow to reach equilibrium because of the slow departure of small anions and cations from the surface film and the slow adsorption of surfactant cations.¹² They hypothesized that the slow approach to an equilibrium surface concentration is due to (1) electrostatic repulsion between the similarly charged surfactant and surface film and (2) slow diffusion of small ions across the hydrophobic and low dielectric film. Kekicheff et al. have also measured forces between CTAB-coated mica surfaces at half the critical micelle concentration.¹³ They find that adsorption takes more than about 8 h to reach a steady state. At the end of this paper, we will describe some morphological changes that occur with time when CTA⁺ adsorbs to mica.

Materials and Methods

Sample Preparation and Characterization. Muscovite mica was freshly cleaved in a laminar-flow cabinet immediately before use. Water was prepared by distillation then passage through a Milli-Q RG system consisting of charcoal filters, ion-exchange media, and a 0.2 μm filter. The resulting water has a conductivity of 18 $\text{M}\Omega\text{ cm}^{-1}$, and a surface tension of 72.4 mJ m^{-2} at 22.0 $^{\circ}\text{C}$. Hexadecyltrimethylammonium bromide (99%, BDH, Poole, UK) was recrystallized three times from a distilled-acetone/water mix. After recrystallization, there was no minimum in a plot of surface tension vs concentration. Hexadecyltrimethylammonium chloride (>95%, TCI, Tokyo, Japan) was recrystallized three times from distilled ethanol. Analytical grade CsBr (Aldrich, Milwaukee), CsCl (Ajax, Australia), KCl (Riedel de Haen, Hanover, Germany), LiCl (BDH, Poole, UK), and LiBr (Merck, Darmstadt, Germany) were used as purchased.

Microscopy. Images were captured with a Nanoscope III AFM (Digital Instruments, CA) using silicon ultralevers (Park Scientific, CA) or silicon nitride nanoprobes (Digital Instruments). The cantilevers were cleaned by irradiation for 40 min ($\sim 9\text{ mW/cm}^2$ at 253.7 nm) in a laminar flow cabinet before use. Unless otherwise stated, the images presented are deflection images (showing the error in the feedback signal) with low integral and proportional gains, and scan rates of about 10 Hz. The only filtering of images was a linear subtraction from each line and the filtering inherent in the feedback loop. Distances in lateral dimensions were calibrated by imaging a standard grid (2160 lines/mm), and distances normal to the surface were calibrated by measuring etch pits (180 nm deep).

Measurements were performed in the temperature range $25 \pm 2\text{ }^{\circ}\text{C}$, at pH 6, and at a surfactant concentration equal to twice the cmc in the absence of salt. Since salt lowers the cmc,¹⁴ the imaged surfaces are all in contact with micellar solutions. Before the images were captured the mica substrate was left to equilibrate in the solution of interest for at least 30 min. Imaging was performed at a repulsive force with the tip separated from the mica by about 3–5 nm. Under this condition

the force on the tip is dominated by the surfactant film and thus the image provides information about the surfactant film.

Surface films in 0.1 mol L^{-1} salt solutions reached a steady-state structure within about 30 min (this is not true for HBr solutions, see ref 21) so they were amenable to routine AFM experiments. The surface films in surfactant-only solutions were very slow to equilibrate and we investigated them over a period of one month. Because of the difficulty in continuing an AFM experiment for long periods of time, long equilibration experiments were performed in a variety of ways:

(1) The solution was left in the AFM for periods from 1 to 7 days.

(2) Substrates were equilibrated in a separate vessel, dried, glued on to a sample holder, then transferred to the AFM and imaged in CTA⁺ solution. Drying was achieved with a stream of nitrogen, with the aim of removing just enough bulk-water to allow gluing to the sample holder. Using this technique, we equilibrated samples for periods from 1 to 4 weeks. Drying the mica probably rearranges the outer layer of the adsorbed bilayer, but not the inner layer where slow exchange is expected to occur. The outer layer can readsorb quickly in CTA⁺ solution. We tested the effect of the drying procedure by equilibrating a sample for just half an hour, drying the sample, then imaging in CTA⁺ solution. This sample produced the same images as a film that was left in CTA⁺ solution in the microscope for half an hour but a different image from a sample that was equilibrated for a week in solution then dried and transferred to the microscope.

(3) Substrates were equilibrated in a separate vessel while clamped between a stainless steel disk and a stainless ring that was 0.4 mm thick. (The steel was passivated in nitric acid to prevent rusting.) The assembly could be removed from solution and transferred to the AFM with a droplet of solution always confined between the ring and the mica. The steel ring precluded the use of an O-ring, so the solution was exposed to air during imaging.

Surfactant plus salt solutions were also investigated by methods (1) and (3), but no changes were observed after about 30 min.

Results and Discussion

Figure 1 shows the structure of CTA⁺ aggregates at the mica surface as a function of CsCl concentration, but at a constant CTA⁺ concentration of 0.0027 mol L^{-1} ($2 \times \text{cmc}$ in the absence of additional salt¹⁵). The force between the tip and the mica substrate is long-range repulsive and has an instability at about 3–3.5 nm, consistent with a surface film that is two molecules thick, and charged. (See Figure 2.) For CTA⁺-only, there is also an instability at about 7.5 nm. The structure is thus two bilayers in the absence of CsCl, cylinders in 0.034 mol L^{-1} mM CsCl, and globular in 0.10 mol L^{-1} CsCl.

This series of structures can be explained in terms of surfactant binding to the mica lattice charge. The surface of muscovite mica has one negative lattice charge per 0.48 nm^2 which, in air, is compensated by K^+ ions.¹⁶ In aqueous solution, these negative lattice sites can exchange cations or remain vacant, so the mica surface has a distribution of cations bound to the lattice sites, and free negative sites (Figure 3a).¹⁷ The distribution is given by the Boltzmann equation and the relative affinity of cations for the surface sites (the Mass Action Model).^{17–19} CTA⁺ can bind to the mica lattice ions, so the mica surface can modify the surfactant-aggregate shape by providing a density of counterions that is different from the equilibrium density at the surface of a micelle in bulk solution. By altering the concentration of CTA⁺ relative to that of other

(8) Manne, S.; Gaub, H. E. *Science* **1995**, *270*, 1480–1482.

(9) Ducker, W. A.; Wanless, E. J. *Langmuir* **1996**, *12*, 5915–5919.

(10) Manne, S.; Schäffer, T. E.; Huo, Q.; Hansma, P. K.; Morse, D. E.; Stucky, G. D.; Aksay, I. A. *Langmuir* **1997**, *13*, 6382–6387.

(11) Yang, H.; Kuperman, A.; Coombs, N.; Mamiche-Afara, S.; Ozin, G. A. *Nature* **1996**, *22*, 703–705.

(12) Chen, Y.-L.; Chen, S.; Frank, C.; Israelachvili, J. J. *Colloid Interface Sci.* **1992**, *153*, 244–265.

(13) Kékicheff, P.; Christenson, H. K.; Ninham, B. W. *Colloids Surf.* **1989**, *40*, 31–41.

(14) Hunter, R. J. *Foundations of Colloid Science*; Oxford University Press: Oxford, 1986; Vol. 1, Chapter 10.

(15) Sepulveda, L.; Cortes, J. J. *Phys. Chem.* **1985**, *89*, 5322–5324.

(16) Gains, G. L.; Tabor, D. *Nature* **1956**, *178*, 1305–1306.

(17) Pashley, R. M. *J. Colloid Interface Sci.* **1981**, *83*, 531–546.

(18) Yates, D. E.; Levine, S.; Healy, T. W. *J. Chem. Soc., Faraday Trans* **1974**, *70*, 1807–1818.

(19) Miklavic, S. J.; Ninham, B. W. *J. Colloid Interface Sci.* **1990**, *134*, 305–311.

(20) Ninham, B. W.; Yaminsky, V. *Langmuir* **1997**, *13*, 2097–2108.

(21) Ducker, W. A.; Wanless, E. J. *Langmuir* submitted for publication.

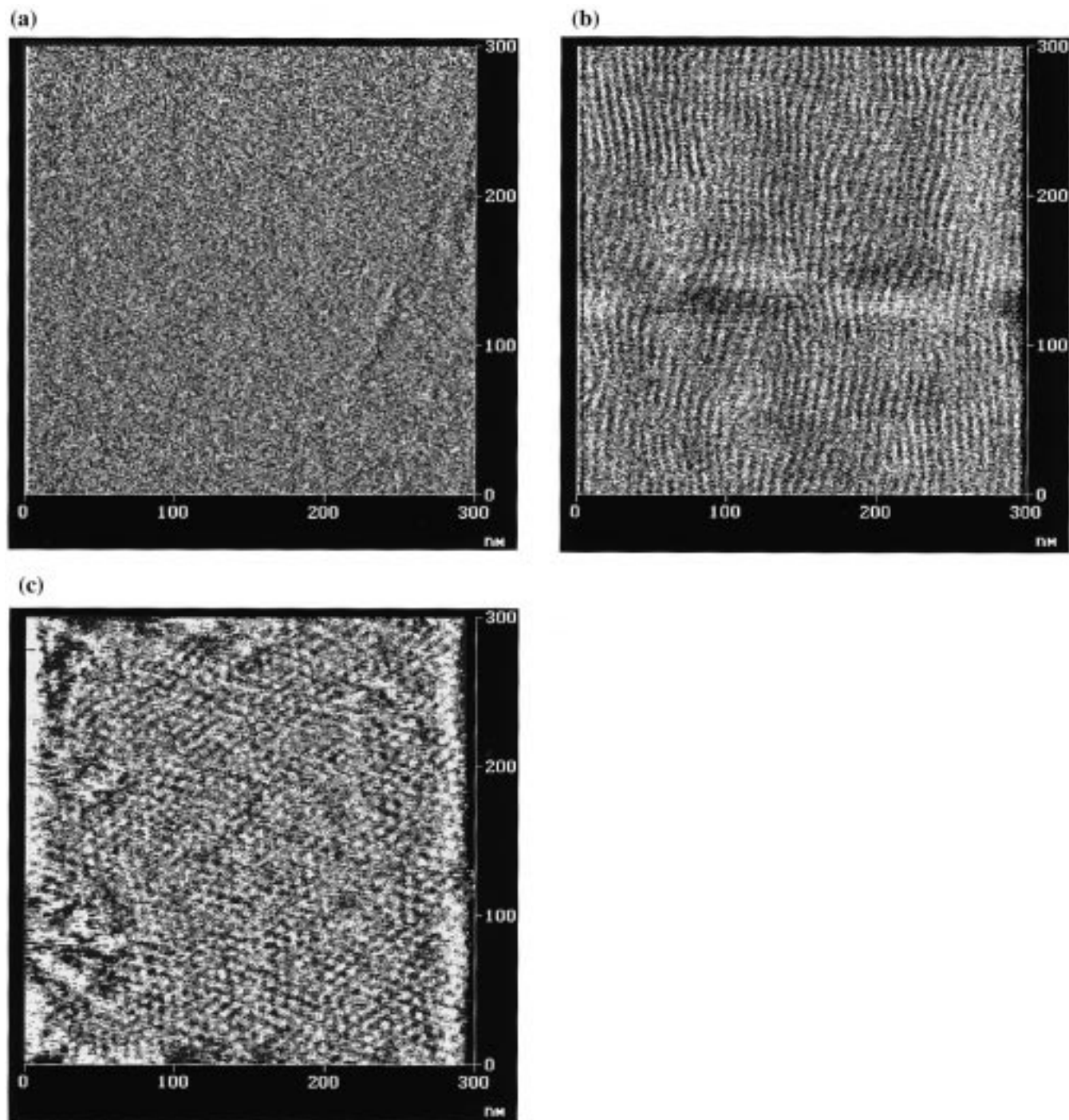


Figure 1. AFM images of CTA^+ aggregates at the interface between muscovite mica and $0.0027 \text{ mol L}^{-1}$ CTAC ($2 \times \text{cmc}$): (a) 0 mol L^{-1} CsCl, a flat layer, consistent with formation of a surfactant bilayer (there are two of these layers); (b) 0.034 mol L^{-1} CsCl, long, thin structures, consistent with cylindrical aggregates; (c) 0.10 mol L^{-1} CsCl, all three aggregate dimensions are similar, consistent with globular aggregates. The flat layer was very slow to reach equilibrium (cf. Figure 7)

cations in bulk solution, we can change the density of surface anions occupied by CTA^+ and thus alter the shape of the surfactant aggregate. It is important to realize that the distance between ions at the interface is very small, so the binding constants of each ion will depend on the concentration of neighboring ions in the film because of electrostatic, dispersion, and other forces. Once a site is occupied by surfactant, neighboring sites are favored for surfactant adsorption because of the hydrophobic effect.

Figure 3 is a schematic showing the role of ion adsorption in determining the surfactant-aggregate shape. When there are few rival cations, the mica surface provides a high density of

counterions in a fixed planar array. This array of anions imposes a planar structure on the adjacent layer of surfactant headgroups (Figure 3b). In addition to the organization introduced by the planar positioning of the anions, the high density of anions also favors a planar structure by screening the repulsive electrostatic interactions between headgroups. A second layer of surfactant associates on top of the first layer to minimize the contact area between the hydrocarbon and water. When a higher concentration of rival cations is introduced, the density of available lattice anions is reduced, and so the spacing between surfactant headgroups increases. The surfactant molecules are also less confined to the plane of the mica surface and more under the

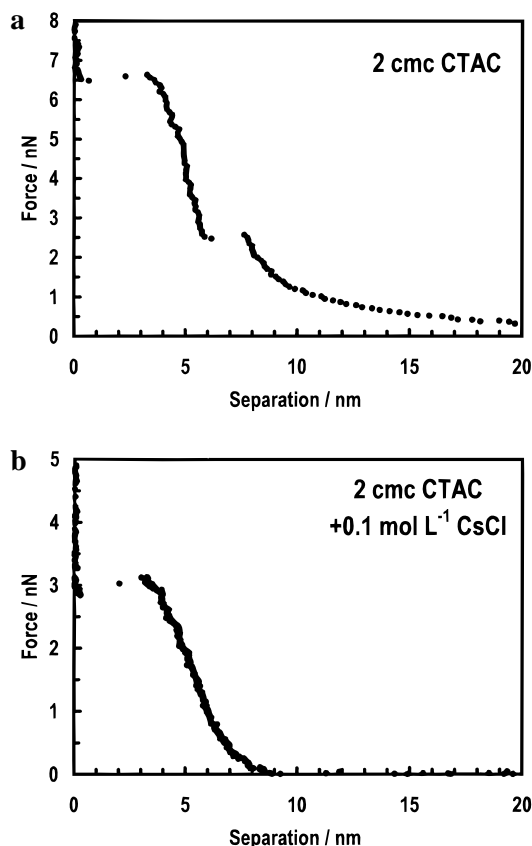


Figure 2. Force acting on an AFM tip as it approaches the mica–solution interface. (a) CTAC-only solution: There is a long-ranged force, which is probably a double-layer force, then a steeper repulsive force followed by an instability at about 7.5 nm separation. The force is consistent with a thin film of surfactant with the headgroups facing the solution. There is another instability at 3–3.5 nm. The positions of the two instabilities are consistent with a surface film consisting of two discrete layers, i.e., two bilayers. (b) CTAC plus 0.1 mol L⁻¹ CsCl: There is now only one layer of surfactant, which is about 3–3.5 nm thick when it is displaced by the tip. There is also a repulsive force suggesting that the headgroups face solution, but the longer-range component is reduced in range. This is consistent with the reduction in solution Debye length from 5.8 nm (a) to 0.94 nm (b).

influence of the mobile anions in solution. In other words, the influence of the mica interface is reduced and the surfactant surface structure becomes more similar to the micellar structure found in bulk solution. Figure 3c shows a schematic of the cylinder cross-section. When the concentration of rival cations is increased further, the density of attachment points for the surfactant decreases further, and the surface aggregate is similar to the bulk aggregate structure, a globular micelle. The alignment of the cylinders may be due to a number of factors: (a) separation-dependent repulsive electrostatic forces between aggregates which favor a constant separation; (b) a maximization of surface coverage; and (c) the existence of energetically preferred attachment sites along a particular orientation relative to the mica crystal.¹¹ (The distance between mica lattice sites (0.5 nm) is much less than the width of the surface aggregates (7 nm) so this mechanism allows some meandering of the cylinders without a high cost in bending.)

To test the surface ion-binding model, we have performed further experiments in which we (1) vary the ratio of CTA⁺ to Cs⁺ concentrations at fixed Cs⁺ concentration, to examine whether the shape is dictated by competition between the two ions, (2) vary the co-ion from Cs⁺ to Li⁺, to examine a co-ion that is more strongly hydrated and thus has a lower affinity for

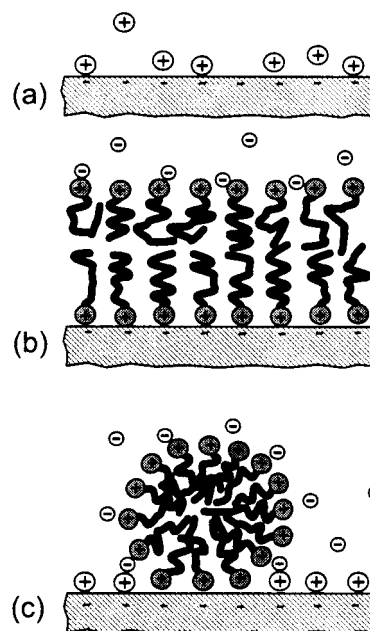


Figure 3. Schematic showing a model for the structure of species adsorbed at the mica–solution interface. The mica has negative lattice sites that can bind cations. (a) When the solution salt (M⁺X⁻) concentration is high and surfactant is absent, most of the lattice sites are occupied by M⁺ ions. (b) When the solution M⁺ concentration is low compared to the surfactant cation concentration, most of the lattice sites are occupied by surfactant cations, and a bilayer is formed. This schematic corresponds to the AFM image in Figure 1a. (c) When the solution M⁺ concentration is high compared to the surfactant cation concentration, M⁺ ions compete with surfactant cations for lattice sites. Many of the lattice sites are now occupied by M⁺ and the surfactant aggregate is only anchored to the surface at a couple of lattice sites (in the cross section). The cylinders in part b have a cross section similar to part c and a long axis similar to part b. The globular micelles in Figure 1c have a cross section like part c in both dimensions. Order in the adsorbed aggregate arises because of organization in the surface lattice sites, and because the hydrophobic effect causes a correlation in the energy of adsorption for neighboring sites.

mica,¹⁷ and (3) vary the counterion, from Cl⁻ to Br⁻, to examine the importance of the strength of binding of the mobile counterion.

Figure 4 shows the structure of CTA⁺ aggregates on mica as a function of CTA⁺ concentration. When we increase the concentration of CTA⁺ from 0.0027 to 0.022 mol L⁻¹, the structure changes from spheres to short cylinders. Thus the structure depends on the ratio of CTA⁺ to Cs⁺, lending support to the mass-action model. However, further refinement of the model is required, because the structure reverts to spheres as the concentration of CTA⁺ is increased further.

Figure 5 shows that CTA⁺ forms disordered cylinders on mica in 0.10 mol L⁻¹ LiCl. The aggregates are much less curved than in 0.10 mol L⁻¹ CsCl (Figure 1c). This is consistent with previously measured binding constants of Cs⁺ and Li⁺ on mica:¹⁹ Li⁺ is a harder ion so has a higher affinity for water. Thus less surface sites are occupied by Li⁺, more sites are occupied by CTA⁺ headgroups, and a lower-curvature structure results. K⁺ has a similar effect to Li⁺. The large difference in effect seen for Cs⁺ and Li⁺ may be partly due to interactions between the cation and the surfactant ion. Cs⁺ is large and polarizable so will have stronger (attractive) dispersion forces than Li⁺ with the surfactant molecules.²⁰

Figure 6 shows the structure of CTA⁺ aggregates in solutions of CTAB plus Br⁻ salts. Comparison to Figures 1 and 5 shows

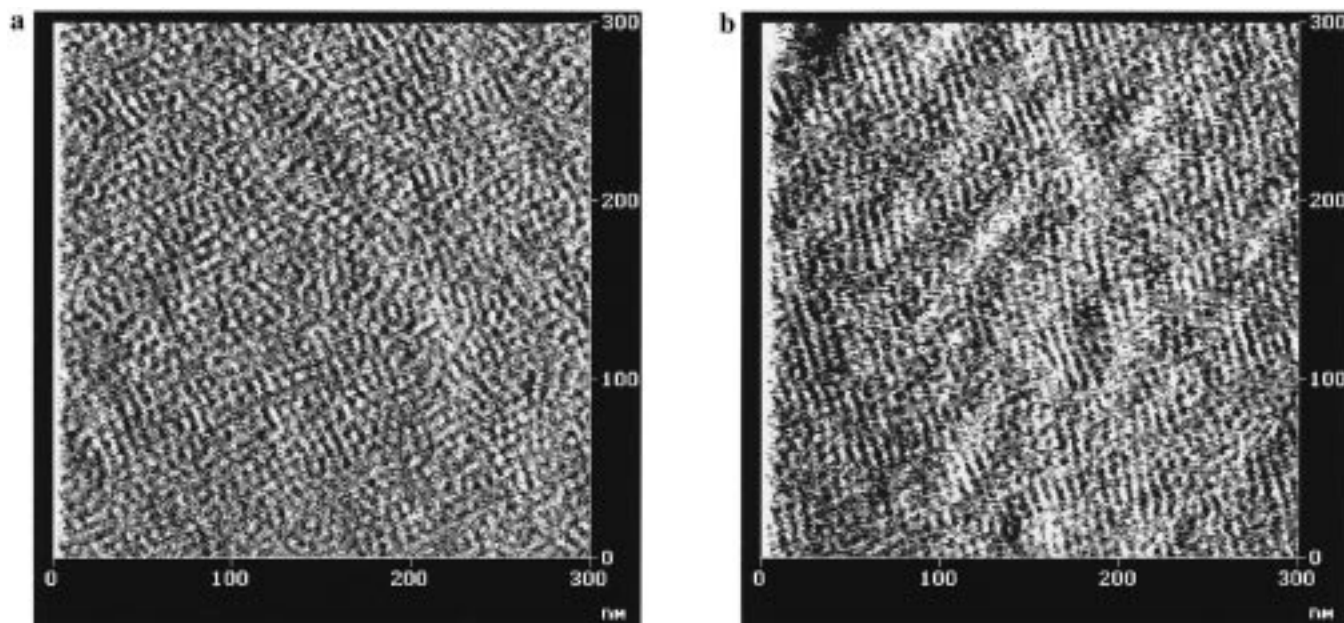


Figure 4. AFM images showing the effect of competition between CTA^+ and Cs^+ ions for lattice sites: (a) $0.0027 \text{ mol L}^{-1}$ CTAC and 0.066 mol L^{-1} CsCl and (b) 0.022 mol L^{-1} CTAC and 0.066 mol L^{-1} CsCl. An increase in CTAC concentration increases the aggregate length in one dimension.

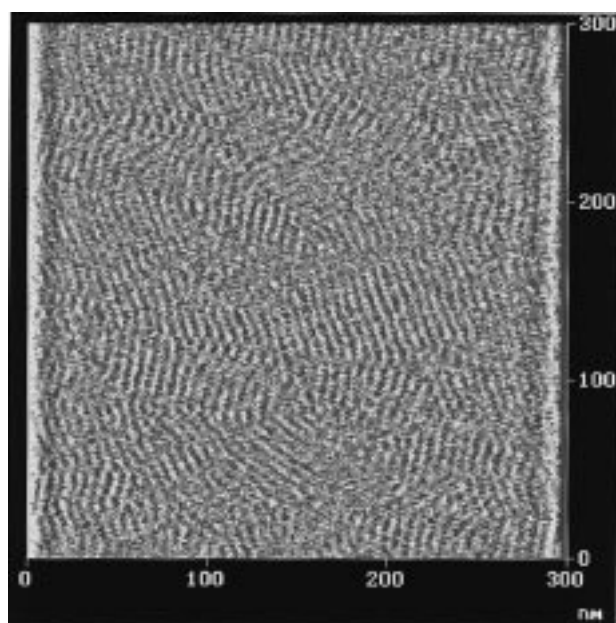


Figure 5. AFM images of CTA^+ aggregates at the interface between muscovite mica and $0.0027 \text{ mol L}^{-1}$ CTAC/ 0.10 mol L^{-1} LiCl solution. Li^+ has a smaller effect than Cs^+ at the same concentration.

the effect of substituting Br^- for Cl^- in the surfactant film. There is little difference between aggregates in 0.10 mol L^{-1} LiBr and 0.10 mol L^{-1} LiCl, but the aggregates formed in CsBr are longer than those in CsCl. The structure in KBr²¹ is more disordered than that in KCl. This is consistent with the observed behavior in bulk solution and with our model. In Li^+ solutions, the concentration of Li^+ at the surface is so low that the surfactant shape is dominated by the mica-lattice counterions and the mobile anion plays a secondary role in determining the aggregate structure. In Cs^+ solutions, the concentration of Cs^+ at the surface is high enough that mobile counterions play a role: the Br^- binds more strongly to the CTA^+ headgroup than Cl^- , and thus reduces headgroup repulsions more, giving a lower aggregate curvature. The schematic in Figure 3c shows the

close proximity of adsorbed M^+ ions and CTA^+ ions for curved surfactant structures; this would only be energetically favored in the presence of counterions.

Finally, we wish to remark on the kinetics of surfactant adsorption. In the presence of 0.10 mol L^{-1} halide salt, we find that the surfactant structures reach a steady state within about 30 min. The observed structures are the same whether the mica is first exposed to the salt or to the surfactant. In surfactant-only solutions, we find that the structure is very slow to equilibrate. This has been observed previously for CTAB by Chen *et al.*¹² They explained the slow equilibration in terms of rapid adsorption of CTAB then slow transport of M^+X^- out of the film.

For CTAB we find that the structures adsorbed initially from $2 \times \text{cmc}$ solutions are cylinders (Figure 7) as described previously,²¹ but that some time between about 6 and 20 h after the mica is exposed to CTAB solution, three changes occur: the structure evolves to (flat) bilayers; a larger force is required to displace the film; and a second, weakly attached bilayer forms on top of the first layer (as previously reported¹³). The initial formation of cylindrical aggregates at the interface is not contingent on the presence of micelles in *bulk* solution: cylinders also form at 0.5 and 0.75 of the cmc. However, in the initial stages of adsorption, the CTA^+ concentration *near the mica* may be above the cmc because of the electrostatic surface potential.²² When observed after one month in $2 \times \text{cmc}$ solutions, the flat sheet structure is retained. Similar behavior is observed for CTAC. This is consistent with our model of rival cations occupying attachment sites of the mica and increasing the curvature of the adsorbed surfactant aggregate: slow transport of salt (HX) out of the film (observed by Chen *et al*) is accompanied by a transition from cylinders to a flat surfactant film. It is not clear whether cylinders displaced by the AFM tip move sideways or out of the film, but an increase in the displacement forces with time implies that the film is more strongly bound to the mica. This is also consistent with the departure of metal cations and binding of more surfactant ions measured by Chen *et al*.

(22) Wangnerud, P.; Jonsson, B. *Langmuir* **1994**, *10*, 3542–3549.

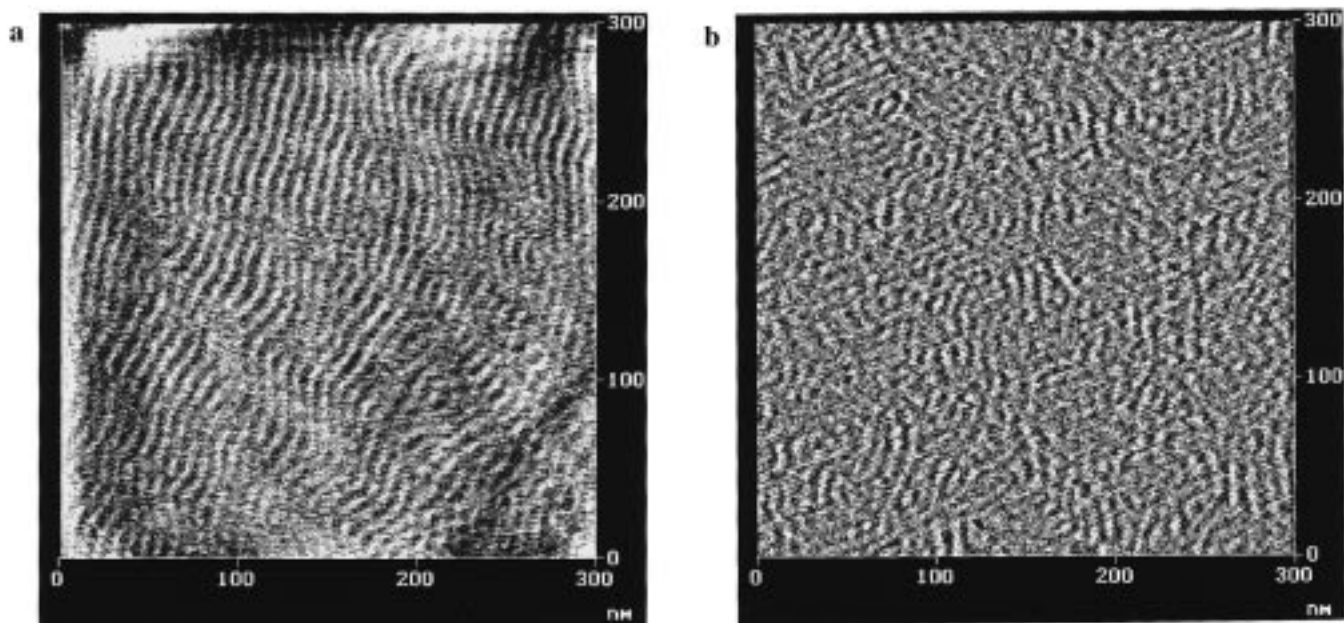


Figure 6. AFM images of CTA^+ aggregates at the interface between muscovite mica and $0.0018 \text{ mol L}^{-1}$ CTAB solution: (a) 0.10 mol L^{-1} LiBr and (b) 0.10 mol L^{-1} CsBr.

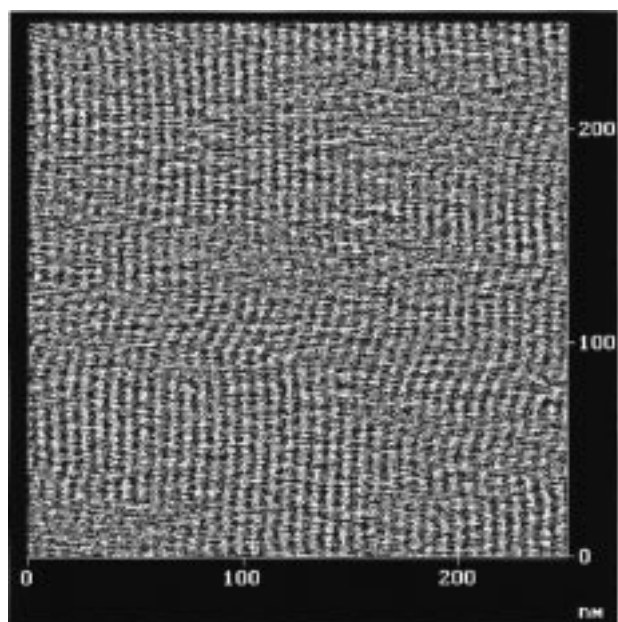


Figure 7. AFM image of CTAB aggregates at the interface between mica and $0.0018 \text{ mol L}^{-1}$ CTAB solution ($2 \times \text{cmc}$) 2 h after the mica was exposed to the CTAB solution.

When the mica sheet is equilibrated in CTAB solution for a week, dried with a stream of nitrogen, and then imaged in CTA^+ solution, the structure is immediately a flat layer that is about 4 nm thick. This shows that the slow process in the cylinder \rightarrow bilayer transformation occurs in the surfactant layer adjacent to the mica surface; equilibration in the outer layer is rapid. As mentioned earlier, a second bilayer forms on top of the first layer for both CTAB and CTAC after about 1 day (total thickness ~ 8 nm). This second layer was removed in the drying process, but we were able to monitor its readsorption. The second layer took several hours to adsorb, and was initially a mosaic of bilayer and cylinder domains. The domains were easily resolved because the cylinders were thicker than the bilayers. With time, many of the cylinder domains evolved into flat sheet (bilayer) structures, as with the first adsorbed layer.

We tried to speed progress to the equilibrium structure by raising the temperature or the pH. When a $2 \times \text{cmc}$ CTAB sample was heated to 32°C the structure transformed from cylinders to a bilayer in 1–2 h. The bilayer structure was retained on cooling to 25°C . Earlier experiments showed that the structure was slow to equilibrate at low pH,²¹ and we suspected that the high charge density of H^+ might inhibit its transport through the film. We thus performed additional experiments at 10^{-4} or $10^{-3} \text{ mol L}^{-1}$ KOH and CTAB to see whether a reduction in the surface H^+ concentration would lead to faster equilibration of the structures. However, we were unable to form bilayers in water in 2 h, at either pH 10 or 11.

Conclusions

The curvature of surfactant aggregates adsorbed to mica can be systematically altered by addition of metal halide salts. Addition of CsCl to CTAC solution causes a transition from a bilayer to cylindrical micelles to globular micelles. These transitions occur in the opposite order to that observed on addition of salt in bulk solution, and at a much lower bulk surfactant concentration. The shape transitions depend on the nature of the salt added. Li^+ has less effect than Cs^+ at the same concentration, and Br^- surfactant aggregates have lower curvature than Cl^- aggregates at the same salt concentration when many mica sites are occupied by metal cations. In surfactant-only solutions, the surface aggregates were very slow to reach an equilibrium structure.

The surface aggregation of CTA^+ is explicable by using two concepts: (1) the binding of counterions to the surfactant aggregate lowers the curvature of aggregate and (2) a high density of surface-bound counterions determines the structure, and promotes a flat surface aggregate, but this influence is diminished by adsorption of co-ions.

Acknowledgment. Our thanks go to Michelle Gee for providing the mica, to George Petersen for providing the ultralevers, to Jacob Israelachvili for a valuable discussion, and to Roe-Hoan Yoon and Herve Marand for the loan of equipment.